Wind Sensorless Control of Wind Energy Conversion System with PMS Generator

Abdelmounime El Magri, Fouad Giri, Abderrahim Elfadili, Luc Dugard

Wind Sensorless Control of Wind Energy Conversion System with PMS Generator

A. El Magri, F. Giri, A. Elfadili, L. Dugard

Abstract— **This paper addresses the problem of controlling wind energy conversion systems (WECS) which involve permanent magnet synchronous generator (PMSG) fed by IGBT-based buck-to-buck rectifier-inverter. The goal of control is to maximize wind energy extraction and this needs letting the wind turbine rotor operate in variable-speed mode. Interestingly, the present study features the achievement of the above energetic goal without resorting to sensors for wind velocity. The control strategy involves: (i) a non-linear regulator designed by the backstepping technique; (ii) a sensorless online reference-speed optimizer designed using the turbine power characteristic to achieve the maximum power point tracking (MPPT) requirement. It is formally shown that the proposed controller actually meets its control objectives. This theoretical result is confirmed by several simulations.**

I. INTRODUCTION

Most wind turbines currently in operation are constrained to work at constant speeds (with a tolerable variation of 1-2%) despite wind speed variations. In such operation conditions, the aerodynamic performance is optimal (in the sense of maximum wind energy extraction) only for one wind speed value depending on the considered value of turbine speed. Achieving maximum wind energy extraction in presence of varying wind speed conditions needs a varying turbine speed operation mode. Specifically, the turbine rotor velocity must be controlled so that its power-speed working point is constantly maintained near the optimal position (Fig. 4). This control objective is commonly referred to 'maximum power point tracking (MPPT)' and its achievement guarantees optimal aerodynamic efficiency.

In this paper, the focus is made on the wind energy conversion system Fig 1. This includes a permanent magnet synchronous generator (PMSG) that converts wind turbine power to output voltage whose amplitude and frequency vary with wind speed. PMSG generators offer several benefits, in wind power applications due to their high power density, high efficiency (as the copper losses in the rotor disappear), and absence of gearbox and reduced active weight. These features make it possible to achieve with PMSG's high varying speed control performance and highly reliable operation conditions (reduced need for maintenance). In the light of the above discussion, the global system including the wind turbine, the PMSG and the AC/DC/AC power converter has to be controlled to achieve accurate reference-speed tracking. The rotor speed reference (ω_{ref}) must be updated online, tacking into account the current wind velocity (v_{win}), so that the MPPT requirement is realized. Existing MPPT methods can be divided in two classes. The first one includes those methods using explicitly the turbine power characteristic, e.g. [1]. The second class includes methods based on extremum-seeking techniques not necessitating the knowledge of turbine characteristics, e.g. [2] [5] [3]. In fact, the required wind speed measurement is a sort of average value of wind speed along the turbine blade. Besides this is not easy to measure, the use of wind sensors entails additional cost and inevitably reduce reliability.

Designing rotor speed reference update laws that are able to meet the MPPT requirement without necessitating wind velocity sensors is a crucial issue that has yet to be solved. A solution is presently developed based on the wind turbine aerofoil characteristic curve. The obtained online speed-reference optimizer represents a key feature of our control strategy which, besides, involves turbine rotor speed regulation, DC link voltage regulation and adaptive state observation. Speed regulation is performed using a nonlinear regulator which, in addition, regulates the d-component of the stator current to zero optimizing thus the delivered stator current. The voltage at the DC link between the AC/DC rectifier and inverter is regulated to a constant reference value (Fig. 2). In fact, the DC link voltage reference value should equal the nominal value of the PMS Generator. This regulation loop controls the reactive power control delivered to the grid. All previous regulation loops are designed using the backstepping technique [8]. The nonlinear multiloop (speed, current, voltage) controller thus obtained (Fig. 3) is formally shown, using Lyapunov stability, to meet its control objectives.

II. MODELING THE ASSOCIATION SYNCHRONOUS GENERATOR-AC/DC/AC CONVERTER

A. Modeling of the combination 'PMSG- DC/AC converter'

The controlled system is illustrated by Fig 1. It includes a combination 'synchronous Generator-rectifier, on one hand, and a tri-phase DC/AC inverter, the other hand. The rectifier is a AC/DC converter operating, like the DC/AC rectifier, according to the known Pulse Wide Modulation (PWM) principle.

Manuscript received September 23, 2011.

A. El Magri, F.Giri, A. and, El Fadili, are with the GREYC Lab, University of Caen, Caen, France

L.Dugard is with GIPSA Lab, ENSIEG, Grenoble, France

Corresponding author: A. El magri, magri_mounaim@ yahoo.fr

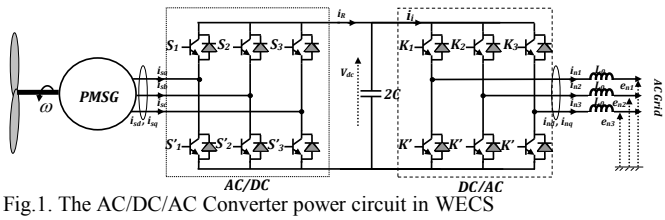

Fig.1. The AC/DC/AC Converter power circuit in WECS

Such modeling is generally performed in the d-q rotating reference frame because the resulting components i_{sd} and i_{sq} turn out to be DC currents. It is shown in [7] that the association PMSG-PWM DC/AC converter model, expressed in the d-q coordinates, can be given by the following state space form:

$$\frac{dx_1}{dt} = -\frac{F}{J}x_1 - \frac{K_M}{J}x_2 + \frac{T_g}{J} \tag{3a}$$

$$\frac{dx_2}{dt} = -\frac{R_s}{L_s}x_2 - p\ x_1 x_3 + \frac{K_M}{L_s}x_1 - \frac{1}{L_s}u_1 v_{dc} \tag{3b}$$

$$\frac{dx_3}{dt} = -\frac{R_s}{L_s}x_3 + p\ x_1 x_2 - \frac{1}{L_s}u_2 v_{dc} \tag{3c}$$

where R_s and L_s are the stator resistor and inductance, J, F, p are the rotor inertia, viscous coefficient and number of poles pairs. T_g is the load torque of the generator, K_M is a flux generator constant. The state variables $x_1 = \overline{\omega}$ is the rotor speed, $(x_2 = i_{sq}, x_3 = i_{sd})$ denote the averaged stator current in dq-coordinate. The inputs control $u_1 = \overline{u}_{sq}, u_2 = \overline{u}_{sd}$ represent the average d- and q-axis of the three-phase duty ratio system (s_1, s_2, s_3). with $(\bar{z})$ denote the average value on the modulation(MLI) period of (z).

B. DC/AC inverter modeling

The inverter circuit (DC/AC) is presented in Fig.1. The power supply net is connected to a converter which consists of a three phase converter that has 6 semiconductors (IGBTs with anti-parallel diodes for bidirectional current flow mode) displayed in three legs 1, 2 and 3. The 6 semiconductors are considered as ideal switches. Only one switch on the same leg can be conducting at the same time.

Applying Kirchhoff's laws, this subsystem is described by the following set of differential equations:

$$L_0 \frac{d}{dt}[i_{n123}] = v_{dc}[k_{123}] - [e_{n123}] \tag{4a}$$

$$2C\frac{dv_{dc}}{dt} = i_r - i_i \tag{4b}$$

$$i_i = [k_{123}]^T [i_{n123}] \tag{4c}$$

where $[i_{n123}] = [i_{n1} \quad i_{n2} \quad i_{n3}]^T$ is the input currents in the electric grid, $[e_{n123}] = [e_{n1} \quad e_{n2} \quad e_{n3}]^T$ is the sinusoidal three-phase net voltages (with known constant frequency ω_n), v_{dc} denotes the voltage in capacitor 2C, i_i designates the input current inverter, and k_i is the switch position function taking values in the discrete set $\{0, 1\}$.

To simplify the three-phase representation (4a) for the synthesis of control laws, the Park transformation is invoked again.

$$\frac{di_{nd}}{dt} = -\frac{1}{L_0}E_{nd} + \omega_n i_{nq} + \frac{1}{L_0}u_{nd}v_{dc} \tag{6a}$$

$$\frac{di_{nq}}{dt} = -\frac{1}{L_0}E_{nq} - \omega_n i_{nq} + \frac{1}{L_0}u_{nq}v_{dc} \tag{6b}$$

$$2C\frac{dv_{dc}}{dt} = i_R - i_i \tag{6c}$$

where (E_{nd}, E_{nq}), (i_{nd}, i_{nq}) and (u_{nd}, u_{nq}) denote the averaged network voltage and current and input control of the inverter in dq-coordinate (Park's transformation).

The power absorbed by the DC/AC converter is given by the well known expression $P_{Load} = i_i v_{dc}$. On the other hand, the power released by the network is given by $P_{OUT} = [e_{n123}]^T [i_{n123}] = E_{nd} i_{nd} + E_{nq} i_{nq}$. Using the power conservation principle, one has $P_{Load} = P_{OUT}$ or, equivalently $i_i v_{dc} = E_{nd} i_{nd} + E_{nq} i_{nq}$. Also, from (6a-b) one gets that:

$$2v_{dc}\frac{dv_{dc}}{dt} = -\frac{1}{C}E_{nd}\,i_{nd} - \frac{1}{C}\left(E_{nq}\,i_{nq} - v_{dc}\,\bar{i}_R\right) \tag{7a}$$

$$\frac{di_{nd}}{dt} = -\frac{1}{L_0}E_{nd} + \omega_n i_{nq} + \frac{1}{L_0}u_{nd}v_{dc} \tag{7b}$$

$$\frac{di_{nq}}{dt} = -\frac{1}{L_0}E_{nq} - \omega_n i_{nd} + \frac{1}{L_0}u_{nq}v_{dc} \tag{7c}$$

Let us introduce the state variables $x_4 = \bar{v}_{dc}^2$, $x_5 = \bar{i}_{nd}$, $x_6 = \bar{i}_{nq}$ and $u_3 = \overline{u}_{nd}, u_4 = \overline{u}_{nq}$ represent the average d-and q-axis components of the three-phase duty ratio system k_i.

The state space equations obtained up to now are put together to get a state-space model of the whole system including the AC/DC/AC converters combined with the synchronous generator. For convenience, the whole model is rewritten here for future reference:

$$\frac{dx_1}{dt} = -\frac{F}{J}x_1 - \frac{K_M}{J}x_2 + \frac{T_g}{J} \tag{9a}$$

$$\frac{dx_2}{dt} = -\frac{R_s}{L_s}x_2 - p\ x_1 x_3 + \frac{K_M}{L_s}x_1 - \frac{1}{L_s}u_1 v_{dc} \tag{9b}$$

$$\frac{dx_3}{dt} = -\frac{R_s}{L_s}x_3 + p\ x_1 x_2 - \frac{1}{L_s}u_2 v_{dc} \tag{9c}$$

$$\frac{dx_4}{dt} = -\frac{1}{C}E_{nd}\,x_5 - \frac{1}{C}\left(E_{nq}\,x_6 - v_{dc}\,\bar{i}_R\right) \tag{9d}$$

$$\frac{dx_5}{dt} = -\frac{1}{L_0}E_{nd} + \omega_n x_6 + \frac{1}{L_0}u_3 v_{cd} \tag{9e}$$

$$\frac{dx_6}{dt} = -\frac{1}{L_0}E_{nq} - \omega_n x_5 + \frac{1}{L_0}u_4 v_{cd} \tag{9f}$$

III. CONTROL OBJECTIVES

There are five operational control objectives:

CO1. Optimization of wind energy extraction: one must determine the optimal reference speed that makes the extracted energy be maximal.

CO2. Speed regulation: the machine speed ω must track a given reference signal ω_{ref}. This reference has been obtained from the MPPT strategy (e.g. [1]).

CO3. The inverter output currents (i_{n1}, i_{n2}, i_{n3}) must be sinusoidal with the same frequency as the supplied power grid and the reactive power in the AC grid must be well regulated.

CO4. Controlling the continuous voltage v_{dc} making it track a given reference signal v_{dcref}. This generally is set to a constant value equal to the nominal voltage entering the converter and machine.

CO5. Regulate the current i_{sd} to a reference value i_{dref}, preferably equal to zero in order to optimize the stator current (see e.g. [12]).

IV. STATE FEEDBACK CONTROLLER DESIGN

A. Wind sensorless rotor speed reference optimization

The optimization strategy is to search a reference speed ω_{opt}, in order to achieve optimal speed ratio working conditions of the wind turbine to capture the maximum energy from the wind. The wind power acting on the swept area of the blade A is a function of the air density ρ (Kg/m^3) and the wind speed v_{win} (m/s). The transmitted power $P(W)$ is generally deduced from the wind power using the power coefficient C_p, as:

$$P = \frac{1}{2} C_p \rho A v_{win}^3 \qquad (10)$$

The power coefficient C_p is a non-linear function of the tip speed-ratio $\lambda = R\omega / v_{win}$ (where R is the turbine radius), which depends on the wind velocity and the rotation speed of the generator rotor ω (rad/s). Fig. 4 represents the transmitted power according to the rotor PMSG speed for various values of the wind speed.

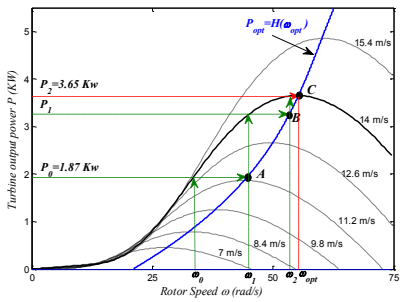

Fig .4 : Turbine Power Characteristics (Pitch angle=0°).

The summits of these curves give the maximum 'extractable' power P_{opt} and so represent the optimal points. Each one of these points is characterized by the optimal speed ω_{opt}. It is readily seen from Fig. 4 that for any wind velocity value, say v_{win}^i, there is a unique couple (ω_i, P_i) that involves the largest extractable power. The set of all such optimal couples (ω_i, P_i) is represented by the blue curve in Fig. 4. A number of such couples have been collected from Fig. 4 and interpolated to get a polynomial function $\omega_{opt} = F(P_{opt})$. Let the obtained polynomial be denoted:

$$F(P) = h_n P^n + h_{n-1} P^{n-1} + \ldots + h_1 P + h_0 \qquad (11)$$

The function $F(.)$ defines the speed-reference optimizer (Fig. 5). Indeed, suppose that, at some instant, the wind velocity is $v_{win}^0 = 14m/s$ and the rotor speed is ω_0. One can see on Fig. 4 which transmitted wind power P_0 corresponds to this couple (v_{win}^0, ω_0). The point is that P_0 is easily online computed. Given only the value of P_0, the speed-reference optimizer gives a new rotor speed reference value $\omega_1 = F(P_0)$. This corresponds to point A on Fig. 4. Assume that, a speed regulator (that has to be determined) is available that makes the machine rotor rotate at the new speed reference i.e. $\omega = \omega_1$. Then, according to Fig. 4, the wind turbine provides a new extractable power value equal to P_1. Then, the speed-reference optimizer will suggest (to the speed regulator) a new speed reference ω_2 (point B). This process will continue until the achievement of the optimal point (P_{opt}, ω_{opt}) (point C on Fig. 4).

B. Speed regulator design for synchronous generator

The regulator design is based on equations (9a-b) where the input signal u_1 stands as the actual input, in order to guarantee speed reference tracking. Following the backstepping technique [8], let z_1 denotes the speed tracking error:

$$z_1 = x_1 - \omega_{ref} = x_1 - x_1^* \qquad (12)$$

In view of (9a), the above error undergoes the following equation:

$$\dot{z}_1 = (-F x_1 - K_M x_2 + T_g)/J - \dot{x}_1^* \qquad (13)$$

In (13), the quantity $\alpha = -(K_M / J) x_2$ stands up as a (virtual) control input for the z_1-dynamics. Let α^* denote the stabilizing function (yet to be determined) associated to α. It is easily seen from (13) that if $\alpha = \alpha^*$ with:

$$\alpha^* = \left(-c_1 z_1 + (F/J) x_1 - (T_g / J) + \dot{x}_1^*\right) (\text{with } c_1 > 0) \qquad (14)$$

Indeed, if $\alpha = \alpha^*$ one will have $\dot{z}_1 = -c_1 z_1$ which clearly is asymptotically stable with respect the Lyapunov function:

$$V_1 = 0.5 z_1^2 \tag{15}$$

In effect, one then has:

$$\dot{V}_1 = z_1 \dot{z}_1 = -c_1 z_1^2 < 0 \tag{16}$$

As $\alpha = -(K_M / J) x_2$, is just a virtual control input, one cannot set $\alpha = \alpha^*$. Nevertheless, the above expression of α^* retained as a first stabilization function and a new error is introduced:

$$z_2 = \alpha - \alpha^* \tag{17}$$

Using (14)-(17), it follows from (13) that the z_1-dynamics undergoes the following equation:

$$\dot{z}_1 = -c_1 z_1 + z_2 \tag{18}$$

The next step consists in determining the control input u_1 so that the (z_1, z_2) error system is asymptotically stable. First, let us obtain the trajectory of the error z_2. Deriving this with respect to time and using (17) gives:

$$\dot{z}_2 = -(K_M / J) \dot{x}_2 - \dot{\alpha}^* \tag{19}$$

Using (14) and (9a-b) in (19), one gets:

$$\dot{z}_2 = \chi(x,t) - c_1^2 z_1 + c_1 z_2 + (K_M / J L_s) u_1 v_{dc} \tag{20}$$

where

$$\begin{aligned} \chi(x,t) = {} & \left(R_s x_2 + p L_s x_1 x_3 - K_M x_1\right)(K_M / J L_s) \\ & + \left(F^2 x_1 + F K_M x_2\right) / J^2 - F T_g / J^2 + \dot{T}_g / J - \ddot{x}_1^* \end{aligned} \tag{21}$$

The error equations (18) and (20) are given in more compact form:

$$\dot{z}_1 = -c_1 z_1 + z_2 \tag{22a}$$

$$\dot{z}_2 = \chi(x,t) - c_1^2 z_1 + c_1 z_2 + (K_M / J L_s) u_1 v_{dc} \tag{22b}$$

To determine a stabilizing control law for (22b), let us consider the quadratic Lyapunov function candidate:

$$V_2 = V_1 + 0.5 z_2^2 = 0.5 z_1^2 + 0.5 z_2^2 \tag{23}$$

Using (18), the time derivative of V_2 can be rewritten as:

$$\dot{V}_2 = -c_1 z_1^2 + z_1 z_2 + z_2 \dot{z}_2 \tag{24a}$$

This shows that, for the (z_1, z_2)-system to be globally asymptotically stable, it is sufficient to choose the control u_1 so that:

$$\dot{V}_2 = -c_1 z_1^2 - c_2 z_2^2 \tag{24b}$$

where $c_2 > 0$ is a new design parameter. In view of (24a), equation (24b) is ensured if:

$$\dot{z}_2 = -c_2 z_2 - z_1 \tag{25}$$

Comparing (25) and (22b) yields the following backstepping control law:

$$u_1 = -J L_s \left((c_1 + c_2) z_2 - (c_1^2 + 1) z_1 + \chi(x,t)\right) / \left(3 K_M v_{dc}\right) \tag{26}$$

C. d-axis current regulation

The d-axis current x_3 undergoes equation (9c) in which the following quantity:

$$v = p x_2 x_1 - u_2 v_{dc} / L_s \tag{27}$$

As the reference signal i_{dref} is null, it follows that the tracking error $z_3 = x_3 - i_{dref}$ undergoes the equation:

$$\dot{z}_3 = -(R_s / L_s) z_3 + v \tag{28}$$

To get a stabilizing control signal for this first-order system, consider the quadratic Lyapunov function $V_3 = 0.5 z_3^2$. It is easily checked that, if the virtual control is let to be $v = -(-R_s / L_s + c_3) z_3$ where $c_3 > 0$, then:

$$\dot{V}_3 = -c_3 z_3^2 \tag{30}$$

which is negative definite. Furthermore, substituting (29) in (28), one gets the closed-loop equation:

$$\dot{z}_3 = -c_3 z_3 \tag{31}$$

Now, it is readily observed that the actual control input is obtained substituting (29) into (27) and solving the resulting equation for u_2. Doing so, one gets:

$$u_2 = \left(c_3 z_3 - \left(R_s / L_s\right) z_3 + p x_2 x_1\right) L_s / v_{dc} \tag{32}$$

From (22a), (25) and (31),it is clear that the subsystem is globally exponentially stable.

D. Reactive power and DC voltage controller

In controlling a PFC, the main objective is to obtain a sinusoidal output current and the injection or extraction a desired reactive power in the electric network. The continuous voltage v_{dc} must track a given reference signal v_{dcref}. These objectives lead to two control loops. The first loop ensures the regulation of the DC voltage x_4 and the second ensures the injection of the desired reactive power.

1) DC voltage loop

Based on equations (9d-e), a first equation involving the control input u_3 will now be designed, using the backstepping technique [8], so that the squared DC-link voltage $x_4 = v_{dc}^2$ tracks well any reference signal $x_4^* \overset{def}{=} v_{dcref}^2 > 0$. As the system (9d-e) is of relative degree 2, the design towards that equation is performed in two steps.

Step 1. Let z_4 denote the speed tracking error:

$$z_4 = x_4 - x_4^* \tag{34}$$

In view of (9d), the above error undergoes the following equation:

$$\dot{z}_4 = -E_{nd} x_5 / C + \beta(x_{i=1..3}, z_{i=1..3}) - \dot{x}_4^* \tag{35}$$

$$\beta(\bullet) = -\{E_{nq}\, x_6 + (J L_s / 3 K_M)((c_1 + c_2) z_2 - c_1^2\, z_1 + \chi(x,t)) x_2 - L_s\,(c_3\, z_3 - (R_s / L_s) z_3 + p\, x_2\, x_1) x_3\} / C$$

In (35), the quantity $\alpha_1 = -E_{nd}\, x_5 / C$ stands up as a (virtual) control input for the z_4-dynamics because the actual control input u_3 act on z_4 indirectly through α_1. Following the backstepping design technique, the Lyapunov function candidate is considered as: $V_4 = 0.5 z_4^2$. Deriving V_4 along the trajectory of (35) yields:

$$\dot{V}_4 = z_4 \dot{z}_4 = -z_4 \left(E_{nd}\, x_5 / C - \beta(x,z) + \dot{x}_4^* \right) \tag{36}$$

This suggests for the (virtual control) α_1 the following control law:

$$\alpha_1^* = -c_4 z_4 - \beta(x,z) + \dot{x}_4^* \tag{37}$$

with $c_4 > 0$ a design parameter. Indeed, substituting α_1^* to $\alpha_1 = -E_{nd}\, x_5 / C$ gives $\dot{V}_4 = -c_4 z_4^2$ which clearly is negative definite in z_4. As α_1 is just a virtual control input, one can not set $\alpha_1 = \alpha_1^*$. Nevertheless, the above expression of α_1^* is retained and a new error is introduced:

$$z_5 = \alpha_1 - \alpha_1^* \tag{38}$$

Using (37), it follows from (35) that the z_4-dynamics undergoes the following equation:

$$\dot{z}_4 = -c_4 z_4 + z_5 \tag{39}$$

Step 2. Now, the aim is to make the couple of errors (z_4, z_5) vanish asymptotically. The trajectory of the error z_5 is obtained by time-derivation of (38) i.e.:

$$\dot{z}_5 = -E_{nd}\, \dot{x}_5 / C + c_4 \dot{z}_4 + \dot{\beta}(x,z) - \ddot{x}_4^* \tag{40}$$

Using (39) and (9d-e) in (40) yields:

$$\dot{z}_5 = \beta_1(x_{i=1\ldots6}, z_{i=1\ldots5}) - \frac{E_{nd}}{C L_0} u_3 v_{cd} \tag{41}$$

With $\beta_1(x,z) = c_4 \dot{z}_4 + \dot{\beta}(x,z) - \ddot{x}_4^* + \frac{E_{nd}^2}{C L_0} - \frac{E_{nd}}{C} \omega_n x_6$

To determine a stabilizing control law for (9d-e), let us consider the quadratic Lyapunov function candidate:

$$V_5 = 0.5 z_4^2 + 0.5 z_5^2 \tag{42a}$$

Using (39)-(41), one gets from (42a) that:

$$\dot{V}_5 = -c_4 z_4^2 + z_5 \left(z_4 + \beta_1(x_{i=1\ldots6}, z_{i=1\ldots5}) - (E_{nd} / C L_0) u_3 v_{cd} \right) \tag{42b}$$

This suggests for the control variable u_3 the following choice:

$$u_3 = \left(c_5 z_5 + z_4 + \beta_1(x_{i=1\ldots6}, z_{i=1\ldots5}) \right) C L_0 / E_{nd} v_{cd} \tag{43}$$

where $c_5 > 0$ is a new design parameter. Indeed, substituting (43) in (42b) yields:

$$\dot{V}_5 = -c_4\, z_4^2 - c_5\, z_5^2 < 0 \tag{44}$$

Now, substituting (43) in (41) one obtains the DC voltage closed-loop control system:

$$\dot{z}_4 = -c_4 z_4 + z_5; \qquad \dot{z}_5 = -c_5\, z_5 - z_4 \tag{45}$$

2) Reactive Power loop

Here, the focus is made on the control objective CO3 that involves the reactive power Q_n which is required to track its reference Q_n^*. The electrical reactive power injected in the grid is given by $Q_n = E_{nd} x_6 - E_{nq} x_5$. To harmonize notation throughout this section, the corresponding tracking error is denoted $z_6 = Q_n - Q_n^*$. It follows from (9e-f) that z_6 undergoes the differential equation:

$$\dot{z}_6 = \beta_2(x_5, x_6) + v_{cd} \left(E_{nd}\, u_4 - E_{nq}\, u_3 \right) / L_0 \tag{46}$$

with, $\beta_2(x_5, x_6) = -\omega_n \left(E_{nd} x_5 + E_{nq} x_6 \right) - \dot{Q}_n^*$.

As the equation (46) is a first order, it can be (globally asymptotically) stabilized using a simple proportional control law:

$$v_{cd} \left(E_{nd} u_4 - E_{nq}\, u_3 \right) / L_0 = -c_6 z_6 - \beta_2(x_5, x_6) \tag{47}$$

with $c_6 > 0$. Then the control law u_4 is given as:

$$u_4 = \left(-L_0 \left(c_6 z_6 + \beta_2(x_5, x_6) \right) / v_{cd} + E_{nq}\, u_3 \right) / E_{nd} \tag{48}$$

It can be easily checked that the dynamic of z_6 undergoes the following equation:

$$\dot{z}_6 = -c_6\, z_6 \tag{49}$$

Then, from (45) and (49), it is clear that the closed loop subsystem is globally exponentially stable and the error vector (z_4, z_5, z_6) converges exponentially fast to zero, whatever the initial conditions.

V. SIMULATION

The closed loop system is simulated, within the Matlab/Simulink environment, using the electro-mechanical characteristics of Table 1. The controller, mathematically defined by (26), (32), (43) and (48) is simulated. The used numerical values for the design parameters are chosen as follows: $c_1 = 7; c_2 = 4.10^4; c_3 = 10^3; c_4 = 40; c_5 = 10^4; c_6 = 2.10^4$ that proved to be suitable. The controller performances will be evaluated in presence of (time-varying) wind velocity . According to the control design, the remaining closed loop inputs are kept constant: $i_{sd\,ref} = 0\ A, V_{dcref} = 700\ V$ and $Q_{n\,ref} = 0\ VAR$.

TABLE I
WECS SYSTEM CHARACTERISTICS

Grid voltage	380V - 220V/50Hz
AC/DC/AC	$L_0 = 1.5$ mH ; C = 22 mF; PMW: 10 KHz .
Synchronous generator	5 kW ; R_s=0.5Ω; L_S=8.5mH, $\varphi_r = 0.576\ Wb$; p=4; J=2.2Nm/rd/s; F= 0.001417 Nm/rd/s
Wind Turbine	*blade radius is 2 m.*

A. *Illustration of optimization strategy*

Fig 8a shows that the wind speed signal reference takes a low, medium and high value (equal to $8.4, 12.6, 14$ and step to $11.2\ m/s$ at times 0, 10, 20 and 30s respectively). With these values of wind speeds, the turbine generates the rotor torque shown in Fig 8b. Block optimization of speed, studied in section 3.2. Referring to the turbine power characteristics (Fig 4), these active powers correspond to optimal values of each wind speeds.

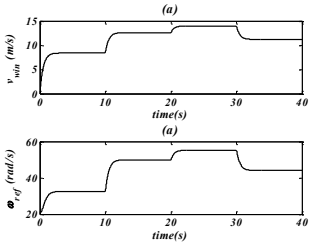

Fig. 8. a) Wind speed; b) Optimized Rotor Speed reference

B. *Illustration of the controller performances*

In this subsection, the controller performances are illustrated by the curves in Fig. 9. Figs 9a and 9b show that the machine speed, $x_1 = \omega$ and the d-component of the stator current, $x_3 = i_{sd}$ perfectly converge to their respective references. The tracking quality is quite satisfactory as the response time (after each change in the wind speed) is less than $1\,s$. Curves (10a) and (10b) respectively show the reactive power injected in the three-phase network Q_n (equals zero) and electric power P_n, produced by the machine and transferred to the grid through the tri-phase inverter.

Fig. 11a shows that the DC-link voltage v_{dc} is tightly regulated: it quickly settles down after each change in the wind speed. The wave frame of the line current i_{n1} is showed in fig 11b. It is seen that the current amplitude changes whenever the wind velocity varies. The current remains (almost) all time sinusoidal and in phase with the network voltage complying with the PFC requirement.

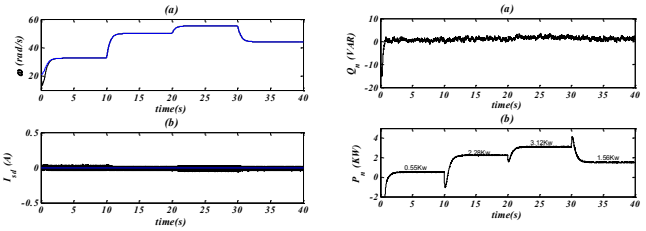

Fig. 9. a) Reference and real rotor speed (m/s); b) d-axis current i_{sd} (A).

Fig. 10. a) Reactive power Q_n (VAR); b) active power P_n (Kw).

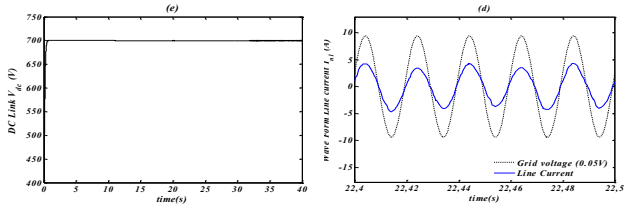

Fig. 11. a) DC link voltage; b) wave frame of the line input current.

VI. CONCLUSION

We have addressed the problem of sensor less control of the wind energy conversion system. Maximum wind energy extraction is achieved by running the wind turbine generator in variable-speed mode without using the sensor wind velocity. The controlled system is an association including wind turbine, permanent magnet synchronous aero-generator and AC/DC/AC converter connected with a tri-phase net work. The system dynamics have been described by the averaged sixth order nonlinear state-space model (9a-f). The multi loops nonlinear controller defined by the control laws (26), (32), (43) and (48) has been designed. The backstepping design technique is used. The controller has been designed to: (i) satisfactory rotor speed reference tracking for extracting maximum power; (ii) tight regulation of the stator d-axis; (iii) power factor correction; (iv) well regulated DC-link voltage (vdc). These results have been confirmed by a simulation study.

REFERENCES

[1] Senjyu T., Ochi Y., Kikunaga Y., Tokudome M., Yona A., Muhando E.B., Urasaki N., Funabashi T., (2009). 'Sensor-less maximum power point tracking control for wind generation system with squirrel cage induction generator', Renewable Energy 34 pp: 994–999, (2009).

[2] Hong Y.-Y., Lu S.-D., Chiou C.-S, (2009). 'MPPT for PM wind generator using gradient approximation', Energy Conversion and Management 50 (1), pp. 82-89, 2009

[3] Kesraoui M., Korichi N., Belkadi A., (2011). 'Maximum power point tracker of wind energy conversion system', Renewable Energy, vol. 36 pp. 2655-2662, (2011)

[4] Boukhezzar B., Siguerdidjane H., (2006), 'Nonlinear Control of Variable-Speed Wind Turbines for Generator Torque Limiting and Power Optimization', J. Sol. Energy Eng., Vol 128, Issue 4, p.516, 2006.

[5] Eftichios K., Kostas K., (2006). 'Design of a Maximum Power Tracking System for Wind-Energy-Conversion Applications', IEEE Transactions on Industrial Electronics, Vol. 53, No. 2, April 2006

[6] Chi S., Zhang Z., Xu L., (2007). 'A novel sliding mode observer with adaptive feedback gain for PMSM Sensorless Vector Control', Power Electronics Specialists Conference, IEEE 2007, pp: 2579-258.

[7] El Magri A., Giri F., Abouloifa A., El fadili A., (2009). 'Nonlinear Control of Associations Including Wind Turbine, PMSG and AC/DC/AC Converters - Speed regulation and power factor correction', IEEE, European Control Conference 2009, August 23-26, 2009, Budapest, Hungary.

[8] Krstic M., Kanellakopoulos I., Kokotovic P., (1995). 'Nonlinear and adaptive control design', John Wilay & Sons, Inc, 1995.

[9] Wallmark O. (2004). 'On control of permanent-magnet synchronous motors in hybrid-electric vehicle application'. Technical Report, School of Electrical Engineering, Chalmers University of technology Goteborg, Sweden.

[10] Michael J, Ryan D., Rik W., (1998). 'Modeling of Sinewave Inverters: A Geometric Approach', Industrial Electronic Conference, IEEE Conference, 1998, vol.1, pp 396 - 401.

[11] Grabic S., Celanovic N., Katic V.A., (2008). ,Permanent Magnet Synchronous Generator Cascade for Wind Turbine Application', Power Electronics, IEEE Transactions, vol 23, May 2008, pp:1136 – 1142

[12] Muhammad H., Rashid, (2001). 'Power electronics handbook', Academic press, 2001.